AIP Advances

RESEARCH ARTICLE | JANUARY 15 2015

Numerical simulation of two dimensional sine-Gordon solitons using modified cubic B-spline differential quadrature method

H. S. Shukla; Mohammad Tamsir; Vineet K. Srivastava

Check for updates

AIP Advances 5, 017121 (2015)
https://doi.org/10.1063/1.4906256

View Online
Export Citation

24 September 2024 03:14:52

AIP Publishing

AIP ADVANCES **5**, 017121 (2015)

Numerical simulation of two dimensional sine-Gordon solitons using modified cubic B-spline differential quadrature method

H. S. Shukla,[1] Mohammad Tamsir,[1,a] and Vineet K. Srivastava[2]
[1]*Department of Mathematics & Statistics, DDU Gorakhpur University, Gorakhpur-273009, India*
[2]*ISRO Telemetry, Tracking and Command Network (ISTRAC), Bangalore-560058, India*

(Received 29 September 2014; accepted 29 December 2014; published online 15 January 2015)

In this paper, a modified cubic B-spline differential quadrature method (MCB-DQM) is employed for the numerical simulation of two-space dimensional nonlinear sine-Gordon equation with appropriate initial and boundary conditions. The modified cubic B-spline works as a basis function in the differential quadrature method to compute the weighting coefficients. Accordingly, two dimensional sine-Gordon equation is transformed into a system of second order ordinary differential equations (ODEs). The resultant system of ODEs is solved by employing an optimal five stage and fourth-order strong stability preserving Runge–Kutta scheme (SSP-RK54). Numerical simulation is discussed for both damped and undamped cases. Computational results are found to be in good agreement with the exact solution and other numerical results available in the literature. © *2015 Author(s). All article content, except where otherwise noted, is licensed under a Creative Commons Attribution 3.0 Unported License.* [http://dx.doi.org/10.1063/1.4906256]

24 September 2024 03:14:52

I. INTRODUCTION

Consider the nonlinear sine-Gordon equation in two dimensional space:

$$\frac{\partial^2 u}{\partial t^2} + \beta \frac{\partial u}{\partial t} = \frac{\partial^2 u}{\partial x^2} + \frac{\partial^2 u}{\partial y^2} - \phi(x, y)\sin(u), \quad x \in R, \quad t \geq 0, \tag{1.1}$$

where $R = \{(x, y) : a \leq x \leq b, \quad c \leq y \leq d\}$, with the suitable initial conditions:

$$\begin{aligned} u(x, y, 0) &= f_1(x, y), \quad (x, y) \in R, \\ \frac{\partial u(x, y, 0)}{\partial t} &= f_2(x, y), \quad (x, y) \in R, \end{aligned} \tag{1.2}$$

and Neumann boundary conditions:

$$\begin{aligned} \frac{\partial u}{\partial n} &= g_1(x, y, t), \quad \text{for } x = a \text{ and } x = b, \quad c \leq y \leq d, \ t \geq 0 \\ \frac{\partial u}{\partial n} &= g_2(x, y, t), \quad \text{for } y = c \text{ and } y = d, \quad a \leq x \leq b, \ t \geq 0. \end{aligned} \tag{1.3}$$

The parameter β is known as the dissipative term with $\beta \geq 0$. Eq. (1.1) reduces to undamped sine-Gordon equation for $\beta = 0$, and to a damped one for $\beta > 0$.

The function $\phi(x, y)$ represents Josephson current density, while $f_1(x, y)$ and $f_2(x, y)$ characterize wave models or kinks and velocity, respectively. The kink operates across the lines or closed curves in the xy-plane, known as the lines and ring soliton waves, respectively. Soliton waves appear in various physical applications such as tsunamis, optical fiber signals, superconductivity,

[a]Corresponding author's email: tamsiriitm@gmail.com

 ©Author(s) 2015

atmospheric waves and gravitational fields with cylindrical symmetry and so on. The simulation of the soliton waves represented by sine-Gordon equation are of the great significance in the field of research. The suitable methods to simulate wave equations successfully has led to a constant demand for achieving the high accuracy. The sine–Gordon equation emerges in the dispersion of fluxons in Josephson junctions, motion of a rigid pendulum, stability of fluid motions, disruptions in crystals etc., refer.[1–5] Josephson junction model[4] consists of two superconducting layers separated by isolated barriers. This model can be described by two-dimensional undamped sine-Gordon equation and has various applications in physics, electronics etc. Djidjeli et al.[7] modeled a soliton-like structure in higher dimensions.

In recent years, various numerical approaches have been developed for the solution of sine-Gordon equation. First of all, Guo et al.[6] proposed two different difference approaches, namely, explicit and implicit schemes. Christiansen and Lomdahl[8] used a generalized leapfrog method for the numerical computation of two-dimensional undamped sine-Gordon equation while a finite element method was used by Argyris et al.[9] Both methods were successfully applied using the appropriate initial conditions with the latter one gave slightly more precise results. Xin[10] used two-dimensional sine–Gordon equation for the modeling of light bullets. Author of Ref. 10 performed a modulation analysis and obseved that sine-Gordon pulse envelopes undergo focusing–defocusing cycles. The evolution of lump and ring solitons of two dimensional sine-Gordon equation and the evolution of standing and travelling breather-type waves were studied in Refs. 11 and 12. However, lump and ring solitons can be applied to Baby Skyrme model and to study the vortex models.[11] Sheng et al.[13] discussed a split cosine method for the numerical simulation of two-dimensional sine-Gordon solitons. Bratsos[15] proposed a modified predictor-corrector approach. In Ref. 16, he introduced the method of lines while a three-time level fourth-order explicit finite-difference method discussed in Ref. 17. An explicit and an improved numerical method to compute the solutions of (2+1) dimension sine-Gordon equation is proposed in Refs. 14 and 18. Dehghan and his colleagues[19–24] proposed number of schemes for the numerical solutions of two-dimensional damped and undamped sine-Gordon equations. In Ref. 19, the authors proposed the dual reciprocity boundary element method and studied the various cases of line and ring solitons of the circular and elliptic shapes. The author of Ref. 20 proposed a numerical scheme based on the collocation points and thin plate splines radial basis functions. In Ref. 21, the author employed a continuous linear element approximation to study the boundary element solution. In Refs. 22–24, the authors proposed various meshless schemes for the numerical solutions of two-dimensional damped and undamped sine-Gordon equations. In Ref. 22, the author presented an implementation of the meshless local boundary integral equation (LBIE) scheme. A local weak meshless scheme based on the radial point interpolation method (RPIM) was proposed in Ref. 23, while a local Petrov–Galerkin (MLPG) method was developed in Ref. 24 by dealing the non-linearity terms by a predictor-corrector scheme with time-stepping scheme for the time derivative. Jiwari et al.[25] introduced a polynomial differential quadrature scheme to solve damped and undamped two-dimensional sine-Gordon equations and discussed various cases involving line solitons and ring solitons.

Differential quadrature technique can be seen in Refs. 26–32 for the solution of the linear and nonlinear one and two dimensional differential equations, while the cubic B-spline and sinc differential quadrature methods can be referred in Refs. 33 and 34. Arora and Singh[35] introduced a new method, namely, a modified cubic B-spline differential quadrature method (MCB-DQM) to solve one dimensional Burger equation and checked its accuracy and efficiency. They claimed that the implementation of this method is straightforward and efficient as compared to other existing numerical methods. Recently, Jiwari and Yuan[36] extended MCB-DQM to show the computational modeling of two-dimensional reaction–diffusion Brusselator model with appropriate initial and boundary conditions. Authors of Refs. 37–39 developed an optimal strong stability preserving (SSP) high order time discretization schemes for the numerical solution of partial differential equations. SSP methods preserve the strong stability properties in any norm, semi norm or convex functional of the spatial discretization coupled with the first order Euler time stepping. They also discussed the description of the optimal explicit and implicit SSP Runge-Kutta and multistep methods. S. Kumar and his colleagues[40–44] solved various partial differential equations analytically. Recently, Shukla

24 September 2024 03:14:52

et al.[45] used the modified cubic B-spline differential quadrature method for solving two dimensional coupled viscous Burger equation.

In this work, we study the numerical simulation of two-dimensional damped and undamped sine-Gordon equation for various cases including line and ring solitons of the circular and elliptic shapes using MCB-DQM. The accuracy and efficacy of the method is confirmed by taking test problem (4.1) of the undamped sine-Gordon equation with Neumann boundary conditions having the exact solution, which shows that MCB-DQM results are acceptable and in good agreement with earlier studies available in the literature. The numerical simulation of damped and undamped sine-Gordon equation is given in the test problems (4.2) to (4.6). Obtained numerical results are compared well with the numerical results available in the literature and a good agreement is achieved. Rest of the article is organized as follows: in Section II, we introduce the modified cubic B-spline differential quadrature method for two dimensional problem. In Section III, implementation process of the method for the test problem (1.1) -(1.3) is illustrated; in Section IV, six numerical examples are discussed to establish the applicability and accuracy, while Section V concludes our study.

II. MODIFIED CUBIC B-SPLINE DIFFERENTIAL QUADRATURE METHOD IN TWO DIMENSION

Firstly, Bellman et al.[26] innovated the differential quadrature method (DQM). In this method, the approximation of the spatial derivatives of a function are computed using the weighted sum of the functional values at the certain discrete points. During the last few years, several kinds of test functions have been used to compute the weighting coefficients such as spline function, sinc function, Lagrange interpolation polynomials, Legendre polynomials, radial basis functions etc., refer.[27–31,33,34] Thereafter, the most generalized approach was proposed by Shu.[32] In this section, description of MCB-DQM[35,36] for the computational solution of sine-Gordon equation in two dimensional space is illustrated. It is supposed that M and N grid points: $a = x_1 < x_2, \ldots, < x_M = b$ and $c = y_1 < y_2, \ldots, < y_N = d$ are distributed uniformly with the spatial step size $\Delta x = x_{i+1} - x_i$ and $\Delta y = y_{j+1} - y_j$ along x and y axis, respectively. According to the method, the first and second order spatial partial derivatives of $u(x, y, t)$ with respect to x (keeping y_j as fixed) and with respect to y (keeping x_i as fixed), are approximated at x_i and y_j, respectively, given by:

$$\frac{\partial u(x_i, y_j, t)}{\partial x} = \sum_{k=1}^{N} w_{ik}^{(1)} u(x_k, y_j, t), \qquad i = 1, 2, \ldots, M \tag{2.1}$$

$$\frac{\partial^2 u(x_i, y_j, t)}{\partial x^2} = \sum_{k=1}^{N} w_{ik}^{(2)} u(x_k, y_j, t), \qquad i = 1, 2, \ldots, M. \tag{2.2}$$

$$\frac{\partial u(x_i, y_j, t)}{\partial y} = \sum_{k=1}^{M} \bar{w}_{jk}^{(1)} u(x_i, y_k, t), \qquad j = 1, 2, \ldots, N \tag{2.3}$$

$$\frac{\partial^2 u(x_i, y_j, t)}{\partial y^2} = \sum_{k=1}^{M} \bar{w}_{jk}^{(2)} u(x_i, y_k, t), \qquad j = 1, 2, \ldots, N, \tag{2.4}$$

where $w_{ij}^{(r)}$ and $\bar{w}_{ij}^{(r)}$, $r = 1, 2$ are the weighting coefficients of the rth-order spatial derivatives with respect to x and y, respectively.

At the knots, the cubic B-spline basis functions[32,45] are considered as:

$$\varphi_m(x) = \frac{1}{h^3} \begin{cases} (x - x_{m-2})^3, & x \in (x_{m-2}, x_{m-1}) \\ (x - x_{m-2})^3 - 4(x - x_{m-1})^3, & x \in (x_{m-1}, x_m) \\ (x_{m+2} - x)^3, & x \in (x_{m+1}, x_{m+2}) \\ 0, & \text{otherwise}, \end{cases} \tag{2.5}$$

24 September 2024 03:14:52

TABLE I. Coefficients of the cubic B-spline φ_m and its derivatives at the node x_m.

	x_{m-2}	x_{m-1}	x_m	x_{m+1}	x_{m+2}
$\varphi_m(x)$	0	1	4	1	0
$\varphi'_m(x)$	0	$3/h$	0	$-3/h$	0
$\varphi''_m(x)$	0	$6/h^2$	$-12/h^2$	$6/h^2$	0

where $\{\varphi_0, \varphi_1, \ldots, \varphi_N, \varphi_{N+1}\}$ is chosen in such a way that it forms a basis over the domain $R = \{(x, y): \ a \le x \le b; \ c \le y \le d\}$. The values of cubic B-spline and its derivatives at the nodal points are depicted in **Table** I.

We modify the cubic B-spline basis functions in such a way that the resulting matrix system of the equations becomes diagonally dominant. The modified cubic B-splines[35] are defined as:

$$\left.\begin{aligned} &\phi_1(x) = \varphi_1(x) + 2\varphi_0(x) \\ &\phi_2(x) = \varphi_2(x) - \varphi_0(x) \\ &\phi_m(x) = \varphi_m(x) \ for \ \mathrm{m} = 3, \ldots, N\text{-}2 \\ &\phi_{N-1}(x) = \varphi_{N-1}(x) - \varphi_{N+1}(x) \\ &\phi_N(x) = \varphi_N(x) + 2\varphi_{N+1}(x) \end{aligned}\right\}, \tag{2.6}$$

where $\{\phi_1, \phi_2, \ldots, \phi_N\}$ forms a basis over the domain $R = \{(x, y): \ a \le x \le b; \ c \le y \le d\}$.

Since, the x-axis is fixed in Eq. (2.1), consequently, by substituting the values of $\phi_m(x)$, $m = 1, 2, \ldots, N$ in Eq. (2.1), we get

$$\phi'_m(x_i) = \sum_{k=1}^{N} w_{ik}^{(1)} \phi_m(x_k), \ \mathrm{i} = 1, 2, \ldots, M. \tag{2.7}$$

With the help of Eq. (2.5), (2.6) and Table I, Eq. (2.7) replaces into a system of linear equations:

$$A\,\vec{w}^{(1)}[i] = \vec{R}[i], \ for \ i = 1, 2, \ldots, M, \tag{2.8}$$

where $\vec{w}^{(1)}[i] = \left[w_{i1}^{(1)}, w_{i2}^{(1)}, \ldots, w_{iN}^{(1)}\right]^T$ is a vector corresponding to x_i, known as weighting coefficient vector, $\vec{R}[i] = \left[\phi'_{1,i}, \ \phi'_{2,i}, \ \ldots \ \ldots, \ \phi'_{N-1,i}, \ \phi'_{N,i}\right]^T$, and the coefficient matrix A is given by:

$$A = \begin{bmatrix} \phi_{1,1} & \phi_{1,2} & & & & & \\ \phi_{2,1} & \phi_{2,2} & \phi_{2,3} & & & & \\ & \phi_{3,2} & \phi_{3,3} & \phi_{3,4} & & & \\ & & \ddots & \ddots & \ddots & & \\ & & & \phi_{N-2,N-3} & \phi_{N-2,N-2} & \phi_{N-2,N-1} & \\ & & & & \phi_{N-1,N-2} & \phi_{N-1,N-1} & \phi_{N-1,N} \\ & & & & & \phi_{N,N-1} & \phi_{N,N} \end{bmatrix} \tag{2.9}$$

The system of linear equations (2.8) is a tridiagonal system. Also, we notice that the coefficient matrix A, being diagonally dominant, is invertible. The system of linear equations (2.8) is solved for each i using the Thomas algorithm. This gives the weighting coefficients $w_{ik}^{(1)}$ of the first order partial derivative. In this way, we obtain the weighting coefficients $w_{ij}^{(2)}$, $1 \le i, j \le N$. The weighting coefficients $w_{ij}^{(2)}$, $1 \le i, j \le N$, are determined by using the formula:[32]

24 September 2024 03:14:52

TABLE II. Comparison of L_∞ and RMS errors for problem (4.1).

	L_∞ – error				RMS-error		
t	Ref. 7	Ref. 20	Ref. 25	present	Ref. 20	Ref. 25	present
1	0.0350	0.0670	0.0027	0.0003	0.0050	0.0005	0.0002
3	0.0431	0.0834	0.0020	0.0006	0.0103	0.00005	0.0004
5	0.0404	0.1015	0.0033	0.0008	0.0145	0.0007	0.0007
7	0.0353	0.1516	0.0059	0.0012	0.0187	0.0011	0.0010

$$\begin{cases} w_{ij}^{(r)} = r\left(w_{ij}^{(1)} w_{ii}^{(r-1)} - \dfrac{w_{ij}^{(r-1)}}{x_i - x_j}\right), \ for\ i \neq j \ \text{and} \ \ i = 1,2,3,\ldots,N; \quad r = 2,3,\ldots,N-1 \\ w_{ii}^{(r)} = -\displaystyle\sum_{j=1, j\neq i}^{N} w_{ij}^{(r)}, \quad \text{for } i = j, \end{cases} \tag{2.10}$$

In the same way, we obtain the weighting coefficients $\bar{w}_{jk}^{(1)}$ of the first order partial derivatives with respect to y by using the modified cubic B-Spline functions in Eq. (2.3). The weighting coefficients $\bar{w}_{ij}^{(2)}$, $1 \leq i, j \leq N$ for the second derivatives can be calculated by the recurrence formule:

$$\begin{cases} \bar{w}_{ij}^{(r)} = r\left(\bar{w}_{ij}^{(1)} \bar{w}_{ii}^{(r-1)} - \dfrac{\bar{w}_{ij}^{(r-1)}}{x_i - x_j}\right), \ for\ i \neq j \ \text{and} \ \ i = 1,2,3,\ldots,N; \quad r = 2,3,\ldots,N-1 \\ \bar{w}_{ii}^{(r)} = -\displaystyle\sum_{j=1, j\neq i}^{N} \bar{w}_{ij}^{(r)}, \quad \text{for } i = j, \end{cases} \tag{2.11}$$

where, the weighting coefficients $w_{ij}^{(r-1)}$, $w_{ij}^{(r)}$, $\bar{w}_{ij}^{(r-1)}$ and $\bar{w}_{ij}^{(r)}$ are correspondig to the $(r-1)^{\text{th}}$ and r^{th} order partial derivatives with respect to x and y, respectively.

III. IMPLEMENTATION OF METHOD TO TWO-DIMENSIONAL SINE-GORDON EQUATION

On substituting the approximate values of the spatial derivatives computed by MCB-DQM, Eq. (1.1) becomes

$$\frac{\partial^2 u(x_i, y_j, t)}{\partial t^2} + \beta \frac{\partial u(x_i, y_j, t)}{\partial t} = \sum_{k=1}^{M} w_{ik}^{(2)} u(x_k, y_j) + \sum_{k=1}^{N} \bar{w}_{jk}^{(2)} u(x_i, y_k) - \phi(x_i, y_j) \sin\left(u(x_i, y_j)\right),$$
$$(x_i, y_j) \in R, \ t > 0, \ i = 1,2,\ldots,M, \quad j = 1,2,\ldots,N, \tag{3.1}$$

together with the initial conditions:

$$\begin{aligned} u(x_i, y_j, 0) &= f_1(x_i, y_j) \\ \frac{\partial u(x_i, y_j, 0)}{\partial t} &= f_2(x_i, y_j). \end{aligned} \tag{3.2}$$

Eq. (3.1) can be replaced into a system of second order differential equations:

$$\frac{d^2 u(x_i, y_j, t)}{dt^2} = L\left(u(x_i, y_j, t)\right), \quad i = 1,2,\ldots,M \ \text{and} \ j = 1,2,\ldots,N, \tag{3.3}$$

The approximation of Neumann boundary conditions (1.3) at $x = a$ and $x = b$ is given as:[25,36]

$$\sum_{k=1}^{M} w_{1,k}^{(1)} u_{k,j} = g_1 \tag{3.4}$$

24 September 2024 03:14:52

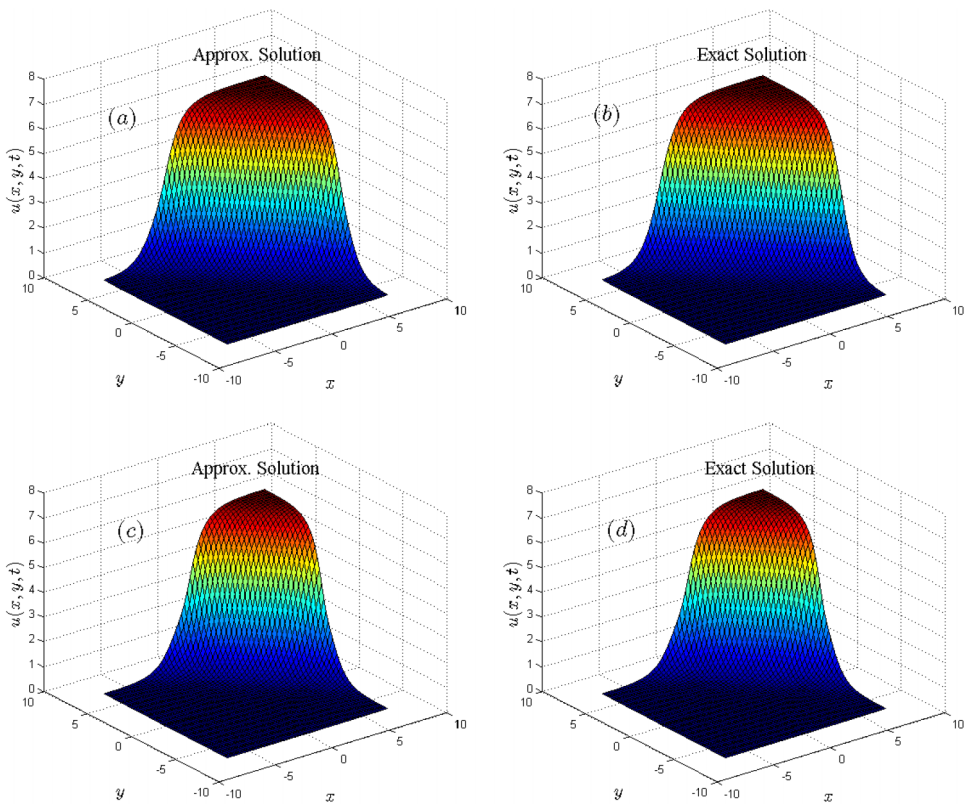

FIG. 1. Simulated and Exact solutions for $t = 5.0$ and $t = 7.0$ with $\Delta t = 0.001$, $\Delta x = \Delta y = 0.25$ for the problem (4.1).

$$\sum_{k=1}^{M} w_{M,k}^{(1)} u_{k,j} = g_2 \tag{3.5}$$

On solving Eqs. (3.4) and (3.5) for $u_{1,j}$ and $u_{M,j}$, we have

$$u_{1,j} = \frac{w_{1,M}^{(1)}(g_2 - S_2) - w_{M,M}^{(1)}(g_1 - S_1)}{\left(w_{1,M}^{(1)} w_{M,1}^{(1)} - w_{1,1}^{(1)} w_{M,M}^{(1)}\right)}, \tag{3.6}$$

$$u_{M,j} = \frac{w_{M,1}^{(1)}(g_1 - S_1) - w_{1,1}^{(1)}(g_2 - S_2)}{\left(w_{1,M}^{(1)} w_{M,1}^{(1)} - w_{1,1}^{(1)} w_{M,M}^{(1)}\right)}, \tag{3.7}$$

where $S_1 = \sum_{k=2}^{M-2} w_{1,k}^{(1)} u_{k,j}$, $S_2 = \sum_{k=2}^{M-2} w_{M,k}^{(1)} u_{k,j}$, $g_1 = g_1(a, y, t)$, $g_2 = g_2(b, y, t)$ and $j = 1, 2, \ldots, N$. Similary, the approximation of Neumann boundary conditions (1.3) at $y = c$ and $y = d$ is given by:

$$\sum_{k=1}^{N} \bar{w}_{1,k}^{(1)} u_{i,k} = g_3(x, c, t), \tag{3.8}$$

$$\sum_{k=1}^{N} \bar{w}_{N,k}^{(1)} u_{i,k} = g_4(x, d, t). \tag{3.9}$$

On solving Eqs. (3.8) and (3.9) for $u_{i,1}$ and $u_{i,N}$, we have

$$u_{i,1} = \frac{\bar{w}_{1,N}^{(1)}(g_4 - S_4) - \bar{w}_{N,N}^{(1)}(g_3 - S_3)}{\left(\bar{w}_{1,N}^{(1)} w_{N,1}^{(1)} - \bar{w}_{1,1}^{(1)} \bar{w}_{N,N}^{(1)}\right)}, \tag{3.10}$$

24 September 2024 03:14:52

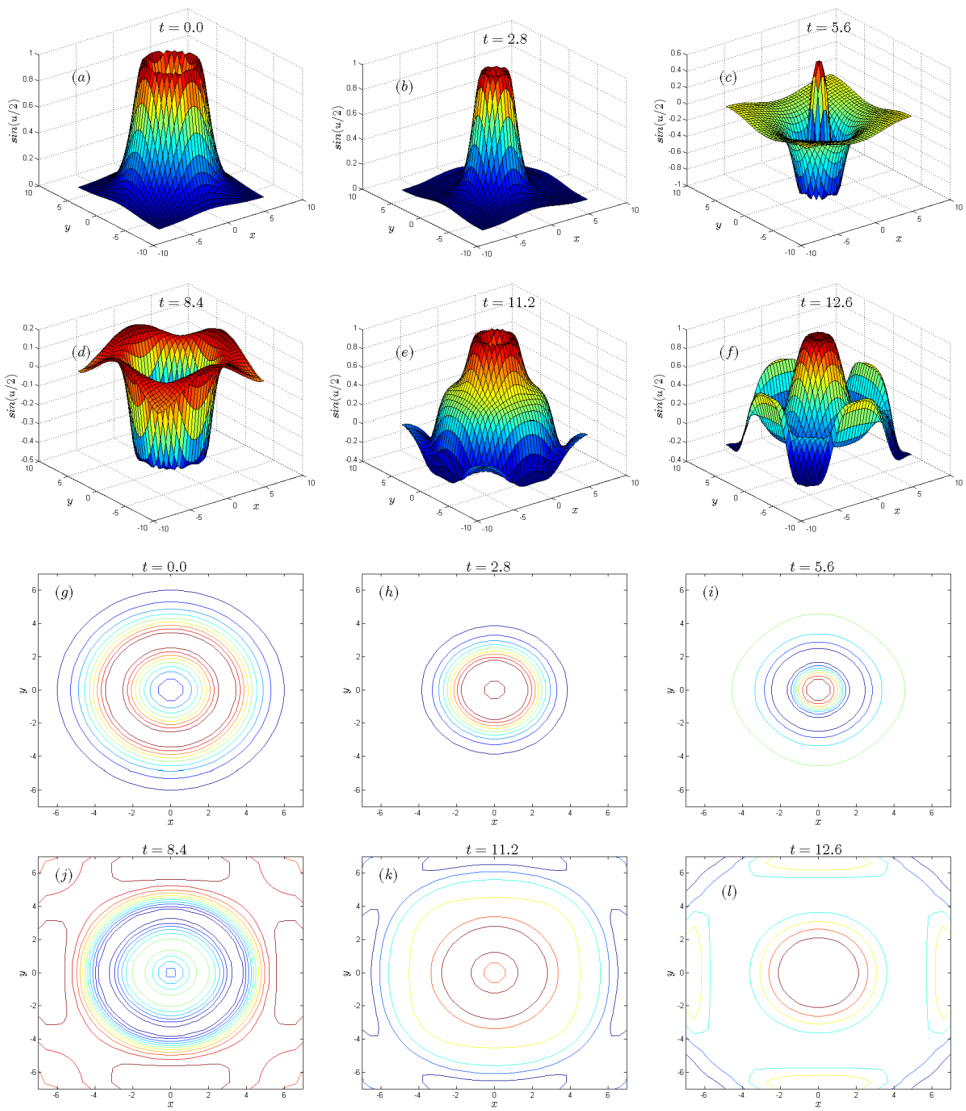

FIG. 2. Initial conditions and Numerical solutions of circular ring solitons at times $t = 2.8, 5.6, 8.4, 11.2, 12.6$ with $\Delta t = 0.2$, $\Delta x = \Delta y = 0.4$ for the problem (4.2).

$$u_{i,N} = \frac{\bar{w}^{(1)}_{N,1}(g_3 - S_3) - \bar{w}^{(1)}_{1,1}(g_4 - S_4)}{\left(\bar{w}^{(1)}_{1,N}\bar{w}^{(1)}_{N,1} - \bar{w}^{(1)}_{1,1}\bar{w}^{(1)}_{N,N}\right)}, \tag{3.11}$$

where $S_3 = \sum_{k=2}^{N-2} \bar{w}^{(1)}_{1,k} u_{i,k}$, $S_4 = \sum_{k=2}^{N-2} \bar{w}^{(1)}_{N,k} u_{i,k}$, $g_3 = g_3(x,c,t)$, $g_4 = g_4(x,d,t)$ and $i = 1, 2, \ldots, M$. The system of second order ordinary differential equations (3.3) together with the initial conditions (3.2) and Neumann boundary conditions (3.6), (3.7), (3.10) (3.11) are solved by SSP-RK54 scheme.

IV. RESULTS AND DISCUSSION

In section, we consider six problems of the line and ring solitons to provide MCB-DQM numerical solutions of Eq. (1.1) with the initial conditions (1.2) and Neumann boundary conditions (1.3). The accuracy and efficiency of the scheme is measured by evaluating the L_∞ and RMS error norms,

24 September 2024 03:14:52

which is given by:

$$\left.\begin{aligned} L_\infty &= \max_{\substack{1\le i\le M\\ 1\le j\le N}} \left| u_{i,j}^{exact} - u_{i,j}^{numerical} \right| \\ \text{and} \quad \text{RMS} &= \frac{1}{M\times N}\sqrt{\sum_{i=1}^{M}\sum_{j=1}^{N}\left|u_{i,j}^{exact} - u_{i,j}^{numerical}\right|^2} \end{aligned}\right\}. \tag{4.1}$$

A. Test problem

In this problem, the numerical solution of Eq. (1.1) is obtained for $\phi(x,y) = -1$ and $\beta = 0$ in the domain $-7 \le x, y \le 7$ with the initial conditions:

$$\left.\begin{aligned} u(x,y,0) &= 4\tan^{-1}(\exp(x+y)), && -7 \le x, y \le 7 \\ u_t(x,y,0) &= -\frac{4\exp(x+y)}{1+\exp(2x+2y)}, && -7 \le x, y \le 7 \end{aligned}\right\} \tag{4.2}$$

and Neumann boundary conditions:

$$\left.\begin{aligned} \frac{\partial u}{\partial x} &= -\frac{4\exp(x+y+t)}{\exp(2t)+\exp(2x+2y)}, && \text{for } x=-7 \text{ and } x=7,\ -7\le y\le 7,\ t>0 \\ \frac{\partial u}{\partial y} &= -\frac{4\exp(x+y+t)}{\exp(2t)+\exp(2x+2y)}, && \text{for } y=-7 \text{ and } y=7,\ -7\le x\le 7,\ t>0 \end{aligned}\right\} \tag{4.3}$$

The exact solution of Eq. (1.1) for $\phi(x,y) = -1$ and $\beta = 0$ with the initial conditions (4.2) is defined as:

$$u(x,y,t) = 4\tan^{-1}(\exp(x+y-t)).$$

This problem is solved numerically in the domain $-7 \le x, y \le 7$ using the parameters: the time step $\Delta t = 0.001$ and space step size $\Delta x = \Delta y = 0.25$. **Table** II shows the L_∞ and root mean square (RMS) error norms at the different time levels $t = 1, 3, 5$ and $t = 7$. From **Table** II, it is seen that the obtained results are comparatively more accurate than those of Refs. 7, 20, and 25. Fig. 1 shows the comparison between the numerical and exact solutions at $t = 5$ and $t = 7$ with $\Delta t = 0.001$ and grid size 31×31. We observe that both results are resemble to each other.

B. Circular ring solitons

The circular ring solitons of two-dimensional sine-Gordon equation (1.1) are obtained for the case $\phi(x,y) = -1$ and $\beta = 0$ in the region $-7 \le x, y \le 7$ with the initial conditions:

$$\left.\begin{aligned} u(x,y,0) &= 4\tan^{-1}\left(\exp\left(3-\sqrt{x^2+y^2}\right)\right), && -7\le x, y\le 7 \\ u_t(x,y,0) &= 0, \quad -7\le x, y\le 7 \end{aligned}\right\} \tag{4.4}$$

and Neumann boundary conditions:

$$\left.\begin{aligned} \frac{\partial u}{\partial x} &= 0, && \text{for } x=\text{-7 and } x=7,\ -7\le y\le 7,\ t>0 \\ \frac{\partial u}{\partial y} &= 0, && \text{for } y=\text{-7 and } y=7,\ -7\le x\le 7,\ t>0 \end{aligned}\right\}. \tag{4.5}$$

Fig. 2 shows the initial conditions and numerical solutions of the circular ring solitons at $t = 2.8, 5.6, 8.4, 11.2$, and $t = 12.6$ in terms of $\sin(u/2)$. Fig. 2 depicts that the ring soliton shrinks from the initial position to $t = 2.8$ and appears as a single ring soliton. The expansion phase starts from $t = 5.6$ and continues until $t = 11.2$, a radiation appears at the beginning of the expansion phase. At $t = 11.2$, a ring soliton is nearly reformed. The graphs depicted in Fig. 2 are in good correspondence with those given in published papers.[7–9,15,18,23,25]

24 September 2024 03:14:52

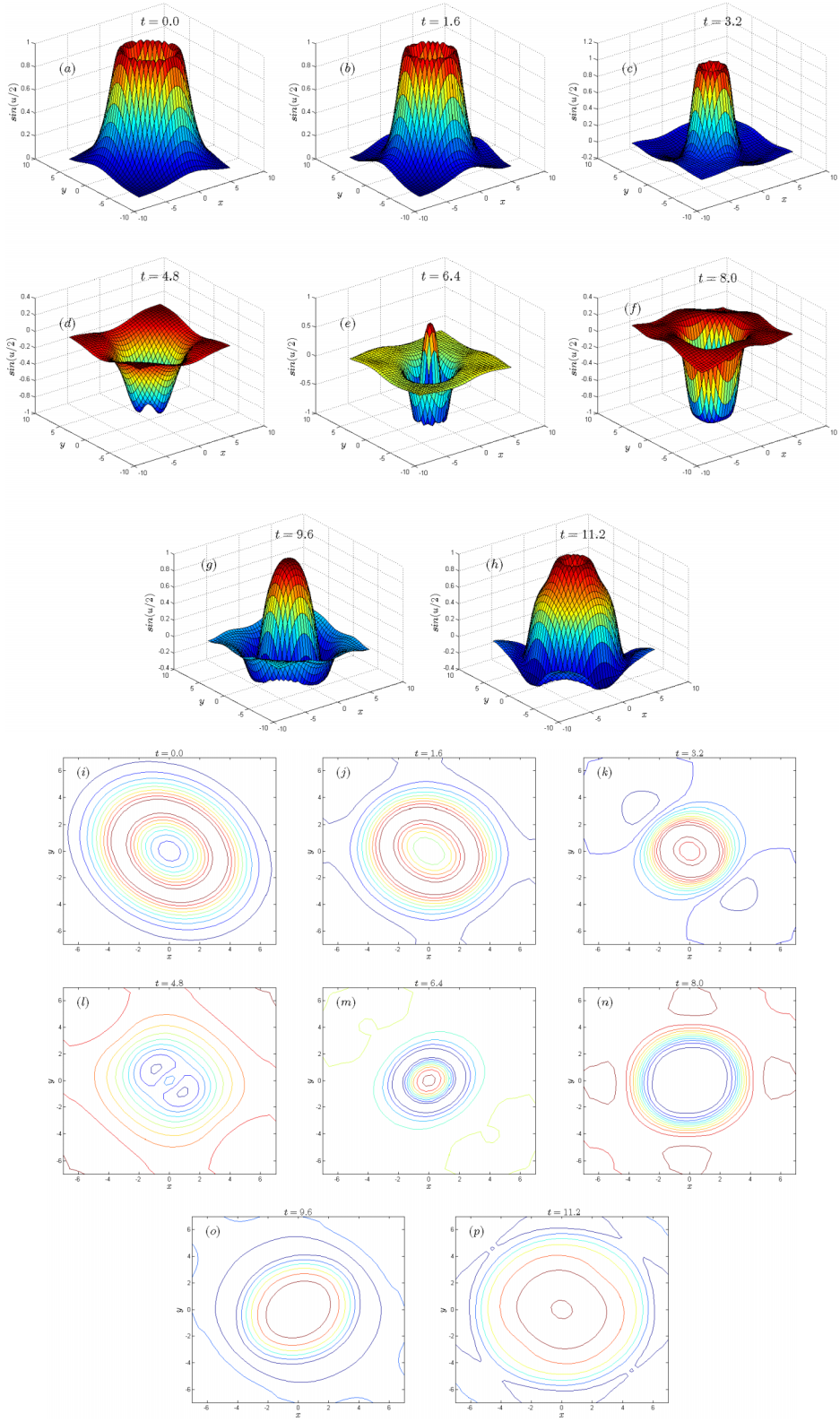

FIG. 3. Initial conditions and Numerical solutions of elliptical ring soliton at times $t = 1.6, 3.2, 4.8, 6.4, 8.0, 9.6, 11.2$ with $\Delta t = 0.2$, $\Delta x = \Delta y = 0.4$ for the problem (4.3).

24 September 2024 03:14:52

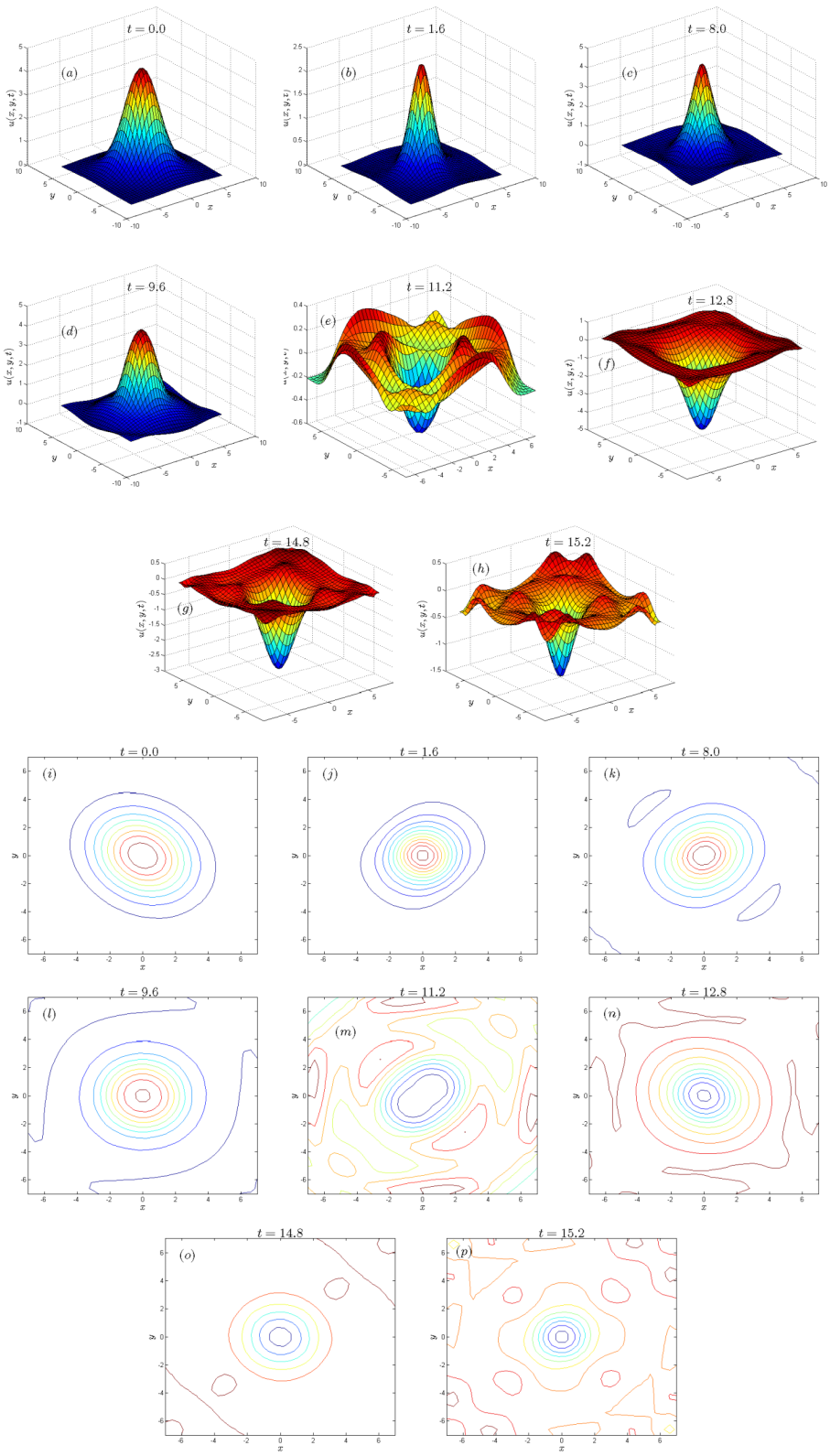

FIG. 4. Initial conditions and Numerical solutions of elliptical breather at times $t = 1.6, 8.0, 9.6, 11.2, 12.8, 14.8, 15.2$ with $\Delta t = 0.2$, $\Delta x = \Delta y = 0.4$ for the problem (4.4).

24 September 2024 03:14:52

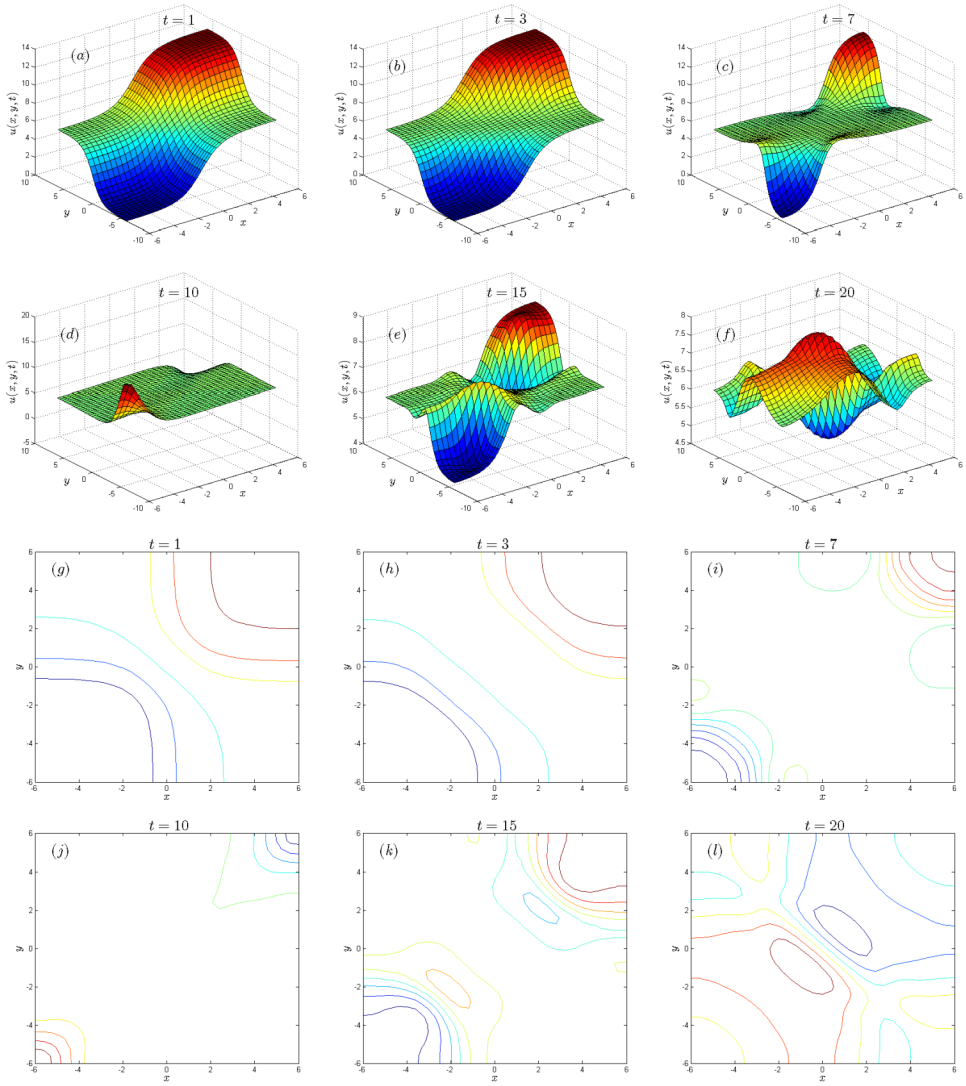

FIG. 5. Numerical solutions of superposition of two orthogonal lines at times $t = 1, 3, 7, 10, 15, 20$ with $\Delta t = 0.001$, $\Delta x = \Delta y = 0.4$ for the problem (4.5).

C. Elliptical ring solitons

The elliptical ring solitons of two-dimensional sine-Gordon equation (1.1) are obtained for the case $\phi(x, y) = -1$ and $\beta = 0$ in the region $-7 \le x, y \le 7$ with the initial conditions:

$$\left.\begin{aligned} u(x, y, 0) &= 4\tan^{-1}\left(\exp\left(3 - \sqrt{\frac{(x-y)^2}{3} + \frac{(x+y)^2}{2}}\right)\right), \qquad -7 \le x, y \le 7 \\ u_t(x, y, 0) &= 0, \qquad -7 \le x, y \le 7 \end{aligned}\right\} \tag{4.6}$$

and Neumann boundary conditions (4.5).

Initial conditions and the numerical solutions of the elliptical ring solitons at $t = 1.6, 3.2, 4.8, 8.0, 9.6, 11.2$ in terms of $\sin(u/2)$ are shown in Fig. 3. From Fig. 3, we notice that the elliptical ring soliton shrinks from its initial position until $t = 3.2$. The temporal behavior of the soliton wave consists of a shrinking and a blowing up phase. From $t = 8.0$, the elliptical ring soliton begins to form a circular ring soliton and at $t = 11.2$, almost a circular ring soliton is seen as given in published papers.[9,16,19,21,23,25]

24 September 2024 03:14:52

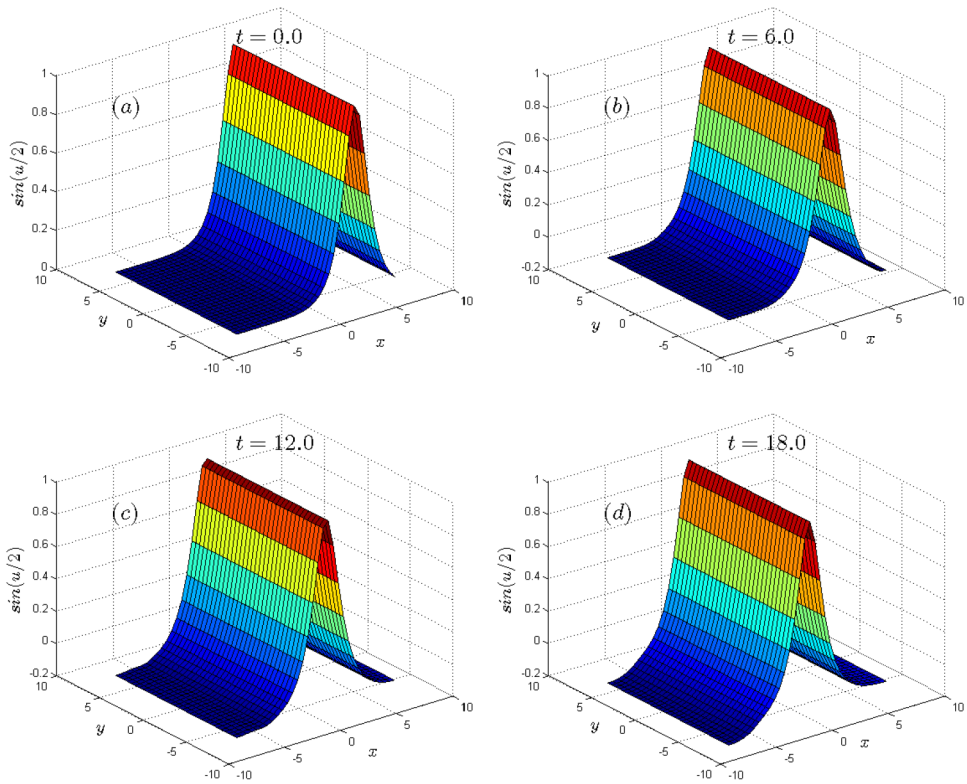

FIG. 6. Initial conditions and Numerical solutions of line soliton in an inhomogeneous medium at times $t = 6.0, 12.0, 18.0$ with $\Delta t = 0.001$ and grid size 31×31 for the problem (4.6).

D. Elliptical breather

In this problem, we consider the elliptical breather for $\phi(x, y) = -1$ and $\beta = 0$ in the domain $-7 \le x, y \le 7$ with the initial conditions:

$$\left.\begin{aligned} &u(x,y,0) = 4\tan^{-1}\left(2.0\sec h\left(0.866\sqrt{\frac{(x-y)^2}{3} + \frac{(x+y)^2}{2}}\right)\right), \qquad -7 \le x, y \le 7 \\ &u_t(x,y,0) = 0, \qquad -7 \le x, y \le 7 \end{aligned}\right\} \tag{4.7}$$

and Neumann boundary conditions (4.5) is discussed.

Fig. 4 depicts the initial condition and numerical solutions and contour plots for the elliptical breather at $t = 1.6, 8.0, 9.6, 11.2, 12.8, 14.8, 15.2$. These graphs reveal that the elliptical breather rotates clockwise from its initial position about the major axis $y = -x$ and shrinks until $t = 1.6$. At $t = 11.2$, the major axis is nearly recovered to its initial position but a stiff oscillation is identified. At $t = 12.8$ an expansion phase begins. A comparison is made between our graphs and the graphs available in the literature. A good agreement is found with those given in Refs. 8, 9, 16, 17, 23, and 25.

E. Superposition of two orthogonal lines

In this problem, the superposition of two orthogonal line solitons are discussed for $\phi(x, y) = -1$ and $\beta = 0.05$ in the region $-6 \le x, y \le 6$ with the following initial conditions:

$$\left.\begin{aligned} &u(x,y,0) = 4\tan^{-1}(\exp(x) + \exp(y)), \qquad -6 \le x, y \le 6 \\ &u_t(x,y,0) = 0, \qquad -6 \le x, y \le 6 \end{aligned}\right\} \tag{4.8}$$

and Neumann boundary conditions (4.5).

24 September 2024 03:14:52

The numerical solutions of this problem are obtained at different time levels $t = 1, 3, 7, 10, 15, 20$ with $\Delta t = 0.001$ and for the grid size 31×31, and are shown in Fig. 5. It can be seen from the graphs that the break up of two orthogonal line solitons at $t = 1$ is found which moves away from each other and a separation occurs between them without any deformation until $t = 3$. At $t = 7$ a deformation is appeared. A good agreement is found with the results given in Ref. 25.

F. Line solitons in an inhomogenous medium

The numerical solutions for a line soliton in an inhomogenous medium are discussed for the case $\phi(x, y) = -1$ and $\beta = 0.05$ in the region $-7 \le x, y \le 7$ with the following initial conditions:

$$\left.\begin{aligned} u(x,y,0) &= 4\tan^{-1}\left(\exp\left(\frac{x-3.5}{0.954}\right)\right), \qquad -7 \le x, y \le 7 \\ u_t(x,y,0) &= 0.629\sec h\left(\exp\left(\frac{x-3.5}{0.954}\right)\right), \qquad -7 \le x, y \le 7 \end{aligned}\right\} \tag{4.9}$$

and Neumann boundary conditions (4.5).

The numerical solutions of this problem in an inhomogeous medium at different time levels $t = 0, 6, 12, 18$ with $\Delta t = 0.001$ and for the grid size 31×31 are depicted in Fig. 6. From Fig. 6, it is clearly seen that the line soliton moves slightly in a straight line during the transmission. A twist appears in its straightness as t increases. Due to the inhomogeneity of the medium, this movement seems to be prevented. Finally, the soliton reforms its straightness at $t = 18$. Christiansen and Lomdahl[8] claimed that this effect is due to the boundary conditions. The graphs are compared with the results of Refs. 20 and 25 and a good agreement is achieved.

V. CONCLUSIONS

In this study, a numerical computation of two-space dimensional damped and undamped sine-Gordon equation is discussed via MCB-DQM, in space and SSP-RK54 scheme, in time. Various cases of the line and ring solitons are discussed together with circular and elliptical shapes. Computed results and graphs are compared with those available in the literature. From the first test problem, it is evident that the described scheme provides more accurate results, and an excellent numerical approximation to the exact solution is achieved. For the rest problems, from the three dimensional and contour plots, it is demonstrated that the scheme gives analogous results as given in the literature. Additionally, it can be noticed that the present scheme provides more accurate results even for small grid sizes.

ACKNOWLEDGMENTS

The authors are thankful to the editor and all reviewers for their valuable comments and suggestions to improve the quality of the paper.

[1] J. K. Perring and T. H. Skyrme, "A model unified field equation," Nucl. Phys. **31**, 550-555 (1962).
[2] G. B. Whitham, *Linear and Nonlinear Waves* (Wiley-Interscience, New York, NY, 1999).
[3] A. Barone, F. Esposito, C. J. Magee, and A. C. Scott, "Theory and applications of the sine-Gordon equation," Rivista del NuovoCimento **1**(2), 227–267 (1971).
[4] J. D. Josephson, "Supercurrents through barriers," Adv. Phys. **14**, 419–451 (1965).
[5] R. K. Dodd, I. C. Eilbeck, and J. D. Gibbon, *Solitons and Nonlinear Wave Equations* (Academic, London, 1982).
[6] B. Y. Guo, P. J. Pascual, M. J. Rodriguez, and L. Vázquez, "Numerical solution of the sine-Gordon equation," Appl. Math. Comput. **18**, 1–14 (1986).
[7] K. Djidjeli, W. G. Price, and E. H. Twizell, "Numerical solutions of a damped sine-Gordon equation in two space variables," J. Eng. Math. **29**, 347–369 (1995).
[8] P. L. Christiansen and P. S. Lomdahl, "Numerical solution of (2 + 1) dimensional sine-Gordon solitons," Physica D **2**, 482–494 (1981).
[9] J. Argyris, M. Haase, and J. C. Heinrich, "Finite element approximation to two dimensional sine-Gordon solitons," Comput. Methods Appl. Mech. Eng. **86**, 1–26 (1991).
[10] J. X. Xin, "Modeling light bullets with the two-dimensional sine-Gordon equation," Physica D **135**, 345–368 (2000).
[11] A. A. Minzoni, N. F. Smythb, and A. L. Worthy, "Pulse evolution for a two-dimensional sine-Gordon equation," Physica D **159**, 101–123 (2001).

24 September 2024 03:14:52

[12] A. A. Minzoni, N. F. Smythb, and A. L. Worthy, "Evolution of two-dimensional standing and travelling breather solutions for the sine–Gordon equation," Physica D **189**, 167–187 (2004).
[13] Q. Sheng, A. Q. M. Khaliq, and D. A. Voss, "Numerical simulation of two-dimensional sine-Gordon solitons via a split cosine scheme," Math. Comput. Simulation **68**, 355–373 (2005).
[14] A. G. Bratsos, "An explicit numerical scheme for the sine-Gordon equation in 2+1 dimensions," Appl. Numer. Anal. Comput. Math. **2**(2), 189-211 (2005).
[15] A. G. Bratsos, "A modified predictor–corrector scheme for the two dimensional sine-Gordon equation," Numer. Algor. **43**, 295-308 (2006).
[16] A. G. Bratsos, "The solution of two-dimensional Sine-Gordon equation using the method of lines," J. Comput. Appl. Math. **206**, 251-277 (2007).
[17] A. G. Bratsos, "A third order numerical scheme for the two-dimensional sine-Gordon equation," Mathematics and Computers in Simulation **76**, 271-282 (2007).
[18] A. G. Bratsos, "An improved numerical scheme for the sine-Gordon equation in (2 +1) dimensions," Int. J. Numer. Meth. Eng. **75**, 787-799 (2008).
[19] M. Dehghan and D. Mirzaei, "The dual reciprocity boundary element method (DRBEM) for two-dimensional sine-Gordon equation," Comput. Methods Appl. Mech. Engrg. **197**, 476–486 (2008).
[20] M. Dehghan and A. Shokri, "A numerical method for solution of the two dimensional sine-Gordon equation using the radial basis functions," Math. Comput. Simulation **79**, 700–715 (2008).
[21] D. Mirzaei and M. Dehghan, "Boundary element solution of the two dimensional sine-Gordon equation using continuous linear elements," Eng. Anal. Boundary Elements **33**, 12–24 (2009).
[22] D. Mirzaei and M. Dehghan, "Implementation of meshless LBIE method to the 2D non-linear SG problem," Int. J. Numer. Methods Engrg. **79**, 1662–1682 (2009).
[23] M. Dehghan and A. Ghesmati, "Numerical simulation of two-dimensional sine-Gordon solitons via a local weak meshless technique based on the radial point interpolation method (RPIM)," Comput. Phys. Comm. **181**, 772–786 (2010).
[24] D. Mirzaei and M. Dehghan, "Meshless local Petrov–Galerkin (MLPG) approximation to the two-dimensional sine-Gordon equation," J. Comput. Appl. Math. **233**, 2737–2754 (2010).
[25] R. Jiwari, S. Pandit, and R. C. Mittal, "Numerical simulation of two-dimensional sine-Gordon solitons by differential quadrature method," Computer Physics Communications **183**, 600-616 (2012).
[26] R. Bellman, B. G. Kashef, and J. Casti, "Differential quadrature: a technique for the rapid solution of nonlinear differential equations," J. Comput. Phy. **10**, 40-52 (1972).
[27] C. Shu and B. E. Richards, "Application of generalized differential quadrature to solve two dimensional incompressible navier-Stokes equations," Int. J. Numer. Meth. Fluids **15**, 791-798 (1992).
[28] J. R. Qan and C. T. Chang, "New insights in solving distributed system equations by the quadrature methods-I," Comput. Chem. Eng. **13**, 779-788 (1989).
[29] J. R. Quan and C. T. Chang, "New insights in solving distributed system equations by the quadrature methods-II," Comput. Chem. Eng. **13**, 1017–1024 (1989).
[30] C. Shu and Y. T. Chew, "Fourier expansion-based differential quadrature and its application to Helmholtz eigenvalue problems," Commun. Numer. MethodsEng. **13**(8), 643–653 (1997).
[31] C. Shu and H. Xue, "Explicit computation of weighting coefficients in the harmonic differential quadrature," J. Sound Vib. **204**(3), 549–555 (1997).
[32] C. Shu, *Differential Quadrature and its Application in Engineering* (Athenaeum Press Ltd, Great Britain, 2000).
[33] A. Korkmaz and I. Dag, "Cubic B-spline differential quadrature methods and stability for Burgers' equation," Eng. Comput. Int. J. Comput. Aided Eng. Software **30**(3), 320–344 (2013).
[34] A. Korkmaz and I. Dag, "Shock wave simulations using sinc differential quadrature method," Eng. Comput. Int. J. Comput. Aided Eng. Software **28**(6), 654–674 (2011).
[35] G. Arora and B. K. Singh, "Numerical solution of Burgers' equation with modified cubic B-spline differential quadrature method," Applied Math. Comput. **224**(1), 166-177 (2013).
[36] R. Jiwari and J. Yuan, "A computational modeling of two dimensional reaction–diffusion Brusselator system arising in chemical processes," J. Math. Chem. **52**, 1535-1551 (2014).
[37] S. Gottlieb, C. W. Shu, and E. Tadmor, "Strong Stability-Preserving High-Order Time Discretization Methods," SIAM REVIEW **43**(1), 89-112 (2001).
[38] J. R. Spiteri and S. J. Ruuth, "A new class of optimal high-order strong stability-preserving time-stepping schemes," SIAM J. Numer. Analysis. **40**(2), 469-491 (2002).
[39] S. Gottlieb, D. I. Ketcheson, and C. W. Shu, "High Order Strong Stability Preserving Time Discretizations," J. Sci. Comput. **38**, 251-289 (2009).
[40] S. Kumar, "A new analytical modelling for telegraph equation via Laplace transform," Applied Mathematical Modelling **38**(13), 3154–3163 (2014).
[41] S. Kumar, "A Numerical Study for Solution of Time Fractional Nonlinear Shallow-Water Equation in Oceans," Zeitschrift fur Naturforschung A **68 a**, 1-7 (2013).
[42] S. Kumar, "Numerical Computation of Time-Fractional Fokker–Planck Equation Arising in Solid State Physics and Circuit theory," Zeitschrift fur Naturforschung **68a**, 1-8 (2013).
[43] S. Kumar and M. M. Rashidi, "New Analytical Method for Gas Dynamics Equation Arising in Shock Fronts," Computer Physics Communications **185**(7), 1947–1954 (2014).
[44] M. M. Khader, S. Kumar, and S. Abbasbandy, "New homotopy analysis transform method for solving the discontinued problems arising in nanotechnology," Chinese Physics B **22**(11), 1-5 (2013).
[45] H. S. Shukla, M. Tamsir, V. K. Srivastava, and J. Kumar, "Numerical solution of two dimensional coupled viscous Burger equation using modified cubic B-spline differential quadrature method," AIP Advances **4**, 117134 (2014).

24 September 2024 03:14:52